applied sciences

MDPI

Article

Smart Public Transport: A Bi-Objective Model for Maximizing Synchronizations and Minimizing Costs in Bus Timetables †

Claudio Risso [1], Sergio Nesmachnow [1,*] and Diego Rossit [2,*]

[1] Facultad de Ingeniería, Universidad de la República, Montevideo 11300, Uruguay; crisso@fing.edu.uy
[2] INMABB, Engineering Department, Universidad Nacional del Sur-CONICET, Bahía Blanca B8000CPB, Argentina
* Correspondence: sergion@fing.edu.uy (S.N.); diego.rossit@uns.edu.ar (D.R.)

† This paper is an extended version of our paper published in V Ibero-American Congress of Smart Cities ISCS CITIES 2022.

Featured Application: The proposed bi-objective model is suitable to provide solutions for the bus synchronization problem to enhance successful transfers in public transportation, considering the cost of the system and the quality of service provided to the users.

Abstract: Modern cities heavily rely on public transport systems to enhance citizen access to urban services and promote sustainability. To optimize public transport, intelligent computer-aided tools play a pivotal role in decision making. This article tackles the complex challenge of bus timetabling, specifically focusing on improving multi-leg trips or transfers. It introduces a novel multi-objective Mixed-Integer Programming Linear (MILP) model that concurrently maximizes passenger transfers and minimizes budgetary costs, while also adhering to the minimum required quality-of-service constraints for regular (non-multi-leg) trips, and an exact resolution approach based on the ε-constraint method to obtain a set of efficient solutions is used. The competitiveness of the model is validated via a computational experimentation performed over real-world scenarios from the public transportation system of Montevideo, Uruguay. The findings evinced that the MILP model was able to compute a set of Pareto efficient solutions that explore the tradeoff between the number of successful transfers and the cost of the system. Moreover, the best tradeoff solutions surpass the current city timetable, excelling in both the number of transfers and cost efficiency.

Keywords: smart public transport; bus timetabling problem; mixed integer programming; bi-objective optimization

Citation: Risso, C.; Nesmachnow, S.; Rossit, D. Smart Public Transport: A Bi-Objective Model for Maximizing Synchronizations and Minimizing Costs in Bus Timetables. *Appl. Sci.* **2023**, *13*, 13032. https://doi.org/10.3390/app132413032

Academic Editor: Juan-Carlos Cano

Received: 30 October 2023
Revised: 23 November 2023
Accepted: 1 December 2023
Published: 6 December 2023

1. Introduction

The paradigm of smart cities involves the development of interconnected and intelligent systems to enhance the livability and sustainability of the cities [1]. Within this framework, a key component is the implementation of smart mobility, which entails designing and operating intelligent transportation networks using cutting-edge technological approaches and effective methods for planning, operation, and management [2].

An emerging problem for decision makers in current cities is the escalating dependence of cars and non-sustainable transportation modes. This upward trend not only has detrimental effects on the environment of the city, including greenhouse gas emissions, visual and noise pollution, and inefficient fuel resource utilization [3–5], but it also contributes to an increased number of road traffic accidents [6]. In order to tackle this issue, the paradigm of smart mobility places a strong emphasis on utilizing public transportation systems [7]. By incorporating efficient vehicles, electric vehicles, and other innovative modes of transportation, it aims to mitigate pollution, alleviate traffic congestion, and address various related challenges. However, in order to encourage citizens to choose public

transportation over private vehicles, the operation of public transport systems must be adapted to the needs of inhabitants [8,9], which requires a careful planning stage of the public transport modes.

Planning and operation of public transport systems involves several decision-making problems including route design, timetabling, and drivers' scheduling, among others [10]. This work focuses on the timetabling problem, i.e., determining bus trip frequencies for a specific operating period [11]. Achieving synchronization of multi-leg (transfer) trips is a critical aspect of the timetabling problem. Synchronization implies ensuring that passengers that have to combine different modes of transport (e.g., different bus lines) to reach their destination have sufficient time to alight from one mode of transport and board the other mode of transport in intermediate stops [12]. Among the diverse modes of transport, the synchronization of timetables of bus lines is widely recognized as a highly complex problem in public transport [13–15]. Experienced public transportation planners and managers often resort to custom intuitive approaches to ensure a satisfactory level of service for citizens. In our previous publications [16–18], we have proposed exact and metaheuristic approaches to address an expanded version of the multi-trips synchronization problem, which takes into account extended transfer zones. This article extends our previous work "Smart mobility for public transport systems: Improved bus timetabling for synchronizing transfers", presented in V Ibero-American Congress of Smart Cities, 2022. The new contents include (i) a new mathematical formulation which aims to simultaneously maximize successful transfers and minimize the budgetary cost; (ii) the implementation of an exact resolution algorithm to solve the bi-objective optimization problem and obtain a set of Pareto efficient solutions; and (iii) an extended experimental evaluation of over 25 problem instances including instances with a diverse number of bus lines based on the city of Montevideo.

This article is organized as described in the following. Section 2 presents the bi-objective Bus Synchronization Problem (BSP), including the main related work, the bus occupation and cost models, and the mathematical formulation. Section 3 describes the proposed methodology for solving the problem. Section 4 presents the computational experimentation, with a description of the implementation details, the instances used, and the main numerical results. Lastly, Section 5 provides a summary of the key findings from this study and suggests potential directions for future research. Table 1 presents the main abbreviations, parameters and variables used in this article.

Table 1. Description of abbreviations and notation used in the article.

	Abbreviations
STM	Metropolitan Transport System of Montevideo
BSP	Bus Synchronization Problem
MILP	Mixed Integer Linear Problem
CT	Current Timetable of Montevideo
QoS	Quality of Service
CO_2	Carbon Dioxide
GPS	Global Positioning System
	Global parameters and variables
$[0, T]$	planning period
	Bus occupation model
ts_i	average daily number of tickets sold for line i
Λ_i	rate at which passengers board buses on line i
L_i	travel distance for passengers on line i
V_i	average speed of buses on line i
td_i	time a passenger spends on a bus before alighting
$T2E_i$	end-to-end travel time for buses on line i
F_i	fixed headway for line i
samples	number of simulations performed

Table 1. *Cont.*

	Cost model
VH	Operating hours of a bus
VKM	Distance traveled by a bus in kilometers
U_{VH}	Unitary cost per operating hour of buses
U_{VKM}	Unitary cost per kilometer traveled by a bus
	Mathematical formulation of Bus Synchronization Problem
H	Set of bus lines
B	Set of transfer zones
R^H	Set of indices of available trips for bus line $h \in H$ along the planning horizon
T	Duration of the planning horizon, measured in minutes.
Dem_b^{hg}	Estimated demand for transfers between lines $h, g \in H$ at transfer zone $b \in B$ during the whole planning horizon.
Co^h	Cost per trip for bus line $h \in H$
Wd_b^{hg}	Time that takes to users to walk between bus stops of bus lines $h \in H$ and $g \in H$ in transfer zone $b \in B$.
Tol_b^{hg}	maximum threshold time that users are willing to wait for a transfer from bus line $h \in H$ to bus line $g \in H$ in a transfer zone $b \in B$.
TT_b^h	Travel time that requires a bus line $h \in H$ to travel from the departure station to transfer zone $b \in B$.
N_h	Minimum number of trips of bus line $h \in H$ to guarantee the quality of service for users who do not transfer.
Hd_h^{min}	Minimum bound for the headway of bus line $h \in H$.
Hd_h^{max}	Maximum bound for the headway of bus line $h \in H$.
a_{rb}^h	Continuous variable that indicates the time when users alight from the trip $r \in R^h$ of bus line $h \in H$ at the transfer zone $b \in B$.
q_r^h	Binary variable that is 1 when trip $r \in R^h$ of line $h \in H$ is to be scheduled.
x_r^h	Continuous variable that indicates the departure time of trip $r \in R^h$ of bus line $h \in H$.
z_{rsb}^{hg}	Binary variable that is 1 when the trip $r \in R^h$ of line $h \in H$ and the trip $s \in R^g$ of line $g \in H$ are synchronized at transfer zone $b \in B$ and 0 otherwise.

2. The Bus Synchronization Problem

This section presents the bi-objective BSP under the operational premises of the city of Montevideo, including the conceptual problem, the tailor-made bus occupation and cost models, the mathematical formulation, and the main related works.

2.1. The Bi-Objective Bus Synchronization Problem in Montevideo

The target problem of this work is based on the public transport system in Montevideo, Uruguay, which is operated under the Metropolitan Transport System (STM) [19]. The STM was implemented to integrate all public transport services in Montevideo and its metropolitan area, including urban agglomerations in nearby departments, namely Canelones and San José. In total, the STM consists of 145 main bus lines, over a thousand line variants, and approximately five thousand bus stops across three departments [20]. These numbers are substantial for a city like Montevideo and emphasize the importance of effective planning to ensure a high-quality service for citizens relying on public transportation. Since its beginning, the STM has introduced various technologies to enhance the efficiency of public transport. One significant advancement was the implementation of a smart card payment system for trips [21,22]. Apart from diverse practical advantages for users, the smart card enables the collection of relevant data and facilitates the extraction

of valuable insights into the mobility patterns of Montevideo's citizens [18]. The STM system stores historical data on the number of trips, ticket sales, GPS records for each bus, and other relevant information [21]. These data have been utilized to develop official and third-party applications that provide accurate information and engage with users.

Passengers using the STM have two main options to reach their destinations. They can choose the traditional "direct" trips, which involve traveling from the origin to the destination without any transfers. Alternatively, passengers can opt for multi-leg trips, also known as transfers [23], within a specified time frame (e.g., one hour or two hours) using the STM card. Within this context, the target Bus Synchronization Problem aims to determine the optimal arrangement of headways (i.e., time intervals between consecutive trips of the same bus line) for each line, in order to simultaneously maximize the number of successful transfers and minimize the cost of the system. Transfers are successful or effective only when two trips are synchronized, i.e., when a passenger has sufficient time to walk from the bus stop from which they alighted the first trip to the stop in which they are going to board the second trip. Additionally, the waiting time at the bus stop for the second trip must not exceed a certain threshold, ensuring a minimum quality of service (QoS) for passengers. Synchronizing transfers is also a very relevant issue in backbone-type networks for public transportation, such as the one proposed for Montevideo [24].

Driving travel times in a urban zone can be highly uncertain since they depend on several aspects (traffic, streets network conditions, weather, etc.). However, by analogy with similar works of the related literature [25,26], the timetabling problem is addressed within a reference interval, during which relevant data for the problem—such as travel times between points and passenger volumes per unit of time—can be considered steady and of uniform distribution. This contributes to simplifying the complex timetabling problem and enables obtaining (near) optimal schedules for a specific period of interest, such as peak hours of the transport system. A particular feature of the model addressed in this work in comparison to others of the related literature is that the model does not assume a predetermined number of trips per line. Instead, the model considers that headways must fall within pre-established minimum and maximum values for each bus line. Additionally, the model guarantees a minimum number of trips per bus line to provide the quality of service for users who do not transfer.

2.2. Bus Occupation Model

Concerning the proposed bus occupancy model, it combines random passenger boarding with deterministic alighting processes. The random boarding process is based on a Poisson distribution, which is a probabilistic distribution that is a commonly used model for random arrivals that are independent and identically distributed [27,28]. Given the assumption of regularity throughout the planning period—during which relevant data for the problem can be considered steady—the Poisson process is considered to have a fixed rate. Consequently, given the average daily number of tickets sold for line i within the planning period $[0, T]$, represented by ts_i, the rate at which passengers board any bus on that line is denoted as $\Lambda_i = ts_i/T$. Λ_i signifies the rate of passengers that any running bus i is expected to pick up, including those who board at any bus stop along the entire set of stops covered by the bus line. The bus occupancy model requires a reference occupancy distribution for each individual bus. By assuming independent passenger arrivals and considering the large number of bus stops, the arrival process at each bus can also be characterized as a Poisson process, and its arrival rate needs to be adjusted to match the overall line's arrival rate. In contrast, the rate of passengers alighting is assumed to be deterministic and constant. Let L_i represent the travel distance for passengers on line i, and V_i represent the average speed of buses on the same line. The time each passenger spends on a bus before disembarking can be calculated as $td_i = L_i/V_i$. All buses on line i commence their trips empty, to pick up passengers along the route. Since the alighting time is fixed at td_i, during the time interval $[0, td_i]$, buses solely receive new passengers (i.e., no passengers disembark during this interval). This interval is referred to as the *ramp-up*

period. The end-to-end travel time for buses on line i, denoted as $T2E_i$, is known because it is calculated from Global Positioning System (GPS) records for each bus. For consistency, the model also assumes a *ramp-down period* at the end, specifically $[T2E_i - td_i, T2E_i]$, during which no new passengers board the bus. Finally, the bus occupancy model assumes fixed headways, represented as F^i, for each line i. If passengers for a particular line are evenly distributed throughout the entire end-to-end travel time, the arrival rate for each bus would be $\Lambda_i \cdot F^i / T2E_i$. However, to maintain the expected number of tickets sold, the rate must be adjusted to $\overline{\Lambda_i} = \Lambda_i \cdot F^i / (T2E_i - td_i)$, taking into account the ramp-down period.

The previous model was implemented using the discrete event simulator as in Algorithm 1, where function *poissrnd* $(\overline{\Lambda_i}, T2E_i - td_i)$ draws $T2E_i - td_i$ samples of independent and identically distributed Poisson random variables of parameter $\overline{\Lambda_i}$. The parameter *Samples* indicates the number of simulations to be performed.

Algorithm 1 Bus Occupation Simulator

Input: $Samples$, T, $\overline{\Lambda_i}$, $T2E_i$, td_i

$busocup \leftarrow \text{zeros}(Samples, T2E_i)$ ▷ A $T2E_i$ minutes simulation per-row
for $\{s \leftarrow 1; s \leq Samples; s{+}{+}\}$ **do**
  $arrivals = \texttt{poissrnd}(\overline{\Lambda_i}, T2E_i - td_i)$ ▷ One Poisson sample per-minute&simulation
  $busoccup(s,1) = arrivals(1)$
  for $\{t \leftarrow 2; t \leq td_i; t{+}{+}\}$ **do** ▷ Ramp-up: arrivals only
    $busoccup(s,t) = busoccup(s,t-1) + arrivals(t)$
  for $\{t \leftarrow td_i{+}1; t \leq T2E_i - td_i; t{+}{+}\}$ **do** ▷ Cruise: arrivals and alightments
    $busoccup(s,t) = busoccup(s,t-1) + arrivals(t) - arrivals(t - td_i)$
  for $\{t \leftarrow T2E_i - td_i{+}1; t \leq T2E_i; t{+}{+}\}$ **do** ▷ Ramp-down: alightments only
    $busoccup(s,t) = busoccup(s,t-1) - arrivals(t - td_i)$

Output: $arrivals \in \mathbb{N}^{Samples, T2E_i}$

A sample distribution of passengers on a bus is illustrated in Figure 1. In this figure, the magenta crosses represent outliers in the sample. It must be ensured that the whiskers of the box plot do not exceed the bus capacity, which is 65 passengers in the given case study. Therefore, for each line i, larger values of F^i are explored until an upper whisker reaches the passenger limit. Let $\overline{F^i}$ represent the maximum headway that respects this requirement for line i. Then, for respecting the capacity of the buses, higher outliers—those located above the upper whiskers—were excluded from consideration.

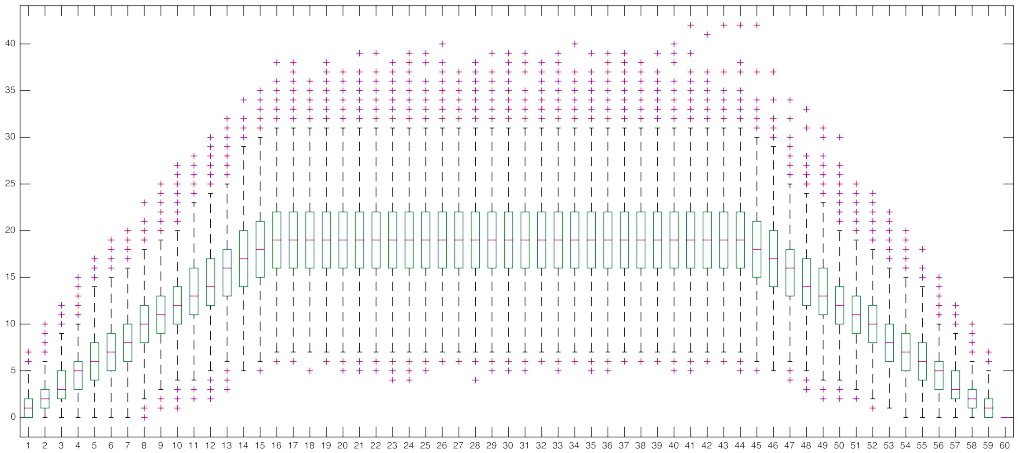

Figure 1. Box plot of an example simulation of the bus occupation along a $T2E_i = 60$ min end-to-end travel with $td_i = 16$ min and $\overline{\Lambda_i} = \frac{9}{8}$ min^{-1}, after $Samples = 10{,}000$ simulations.

2.3. The Cost Model

As aforementioned, the proposed model considers two different objectives: the number of successful transfers and the cost of the system. For estimating the cost of the system, several aspects of the case study are taken into account.

The local authorities in Montevideo conduct regular analyses of the expenses related to the bus system to calculate the kilometer-based fare. This information is utilized to determine the level of state subsidies allocated to the system. Various types of subsidies are applied for public transportation in Montevideo, with two being particularly noteworthy [29]. The first type involves a discounted fuel price that benefits the bus system, whereas the second type entails reduced fares for specific user groups such as students, those retired, and commuters who travel to and from their destinations on a consistent basis. These subsidies have a substantial impact on the cost structure of the system. For instance, the discounted fuel price significantly reduces the cost burden in comparison to other bus systems. In Montevideo, it accounts for only 5% of the total estimated cost [30], as opposed to 13% in comparable public transportation systems [31]. Nevertheless, the discounted fuel price poses a significant cost for the Uruguayan government. Recently, Montevideo has initiated a shift from diesel to electric buses as part of an environmentally conscious approach [5]. The primary objective of this shift is to decrease fossil fuel consumption and mitigate greenhouse gas emissions.

The two primary expenses in the system consist of the driver's salary and the cost of fuel or electricity, depending on the type of bus (diesel or electric). These costs correspond to the operating hours (U_{VH}) for the driver's salary and the distance traveled (U_{VKM}) for fuel or electricity expenses.The driver's salary totals 9.2 USD per hour, which encompasses an 8 USD basic wage along with 1.2 USD in social charges. In term of fuel, the average consumption for a standard diesel bus operating in Montevideo is 0.396 L per kilometer, with the fuel price in the city being approximately 1.6 USD per liter.

The costs models considered for public transportation varies according to their distinct objectives [31]. In this article, the focus is on the problem of determining bus schedule headways without affecting the layout of the bus lines. In cases where the bus line layout remains fixed, the cost functions generally are composed of linear combinations of several unit costs for relevant parameters, such as the bus operating time and the distance traveled [32–34]. Although more complex models can be devised, practitioners also commonly employ these linear functions since they are simple to understand and use in the decision-making process [35]. Hence, this article employs a cost function that is associated with vehicle operating time and distance-traveled variables.

Regarding vehicle operating time, certain operating costs (driver salaries and administrative supervision hours) are directly associated with the number of vehicle operating hours. Consequently, these expenses are appropriately distributed based on vehicle hours. Moreover, vehicle hours are frequently utilized as a proxy for the working hours of employees in cost models, due to their simplicity of calculation [36].

Regarding vehicle distance, several operating costs, including fuel, oil, tires, and vehicle maintenance, are directly related to the distance traveled by buses. Operating costs are determined based on statistical information about operating time and distance traveled [37]. Some linear cost models incorporate the number of buses on the system [33] or consider the number of vehicles needed to meet peak-hour demand, which differs from the demand in off-peak periods [36]. The proposed model focuses on studying time windows during peak hours, assuming a fixed fleet size. Furthermore, the examined case study corresponds to a system with a relatively stable fleet size, as new buses are acquired every five years or even longer. The employed cost function is given as $Cost = U_{VH} \cdot VH + U_{VKM} \cdot VKM$, with VH representing operating hours and VKM the distance traveled by buses. U_{VH} denotes the hourly unit costs, and U_{VKM} denotes the unit costs per kilometer.

2.4. Mathematical Formulation

An assumption that is made is that during the planning horizon T, some relevant data remain stable and follow a uniform distribution. For example, travel times. However, travel times are generally affected by special conditions, such as traffic or street blockades, due to repair works or special fairs (e.g., fairs of food producers which are usual in Montevideo). In this model it is considered constant for the planning period, which is a usual convention in planning problems. Another relevant aspect is that demand for transfers is uniform throughout the planning horizon.

For defining the mathematical formulation of the bi-objective BSP, the following sets, parameters, and variables are used.

Sets

H = set of bus lines. The routes of buses are fixed and known in advance.
B = set of transfer zones. A transfer zone is a geographic area that includes two nearby bus stops from different bus lines.
R^h = set of indices of available trips for bus line $h \in H$ along the planning horizon.

Parameters

T = duration of the planning horizon, measured in minutes.
Dem_b^{hg} = the estimated demand for transfers between lines $h, g \in H$ at transfer zone $b \in B$ during the whole planning horizon. Demand is uniform throughout that period.
Co^h = cost per trip for bus line $h \in H$.
Wd_b^{hg} = time that takes for users to walk between bus stops of bus lines $h \in H$ and $g \in H$ in transfer zone $b \in B$.
Tol_b^{hg} = maximum threshold time that users are willing to wait for a transfer from bus line $h \in H$ to bus line $g \in H$ in transfer zone $b \in B$.
TT_b^h = travel time that requires bus line $h \in H$ to travel from the departure station (beginning of the line) to transfer zone $b \in B$.
N_h = minimum number of trips of bus line $h \in H$ to guarantee the quality of service for users who do not transfer.
Hd_h^{min} = minimum bound for the headway of bus line $h \in H$.
Hd_h^{max} = maximum bound for the headway of bus line $h \in H$.

Variables

a_{rb}^h = (continuous) time when users alight from the trip $r \in R^h$ of bus line $h \in H$ at the transfer zone $b \in B$.
q_r^h = (binary) 1 when trip $r \in R^h$ of line $h \in H$ is to be scheduled.
x_r^h = (continuous) departure time of trip $r \in R^h$ of bus line $h \in H$.
z_{rsb}^{hg} = (binary) 1 when the trip $r \in R^h$ of line $h \in H$ and the trip $s \in R^g$ of line $g \in H$ are synchronized at transfer zone $b \in B$ and 0 otherwise.

A relevant feature is that the model does not assume a predefined number of trips per bus line. Although there is a maximum number of possible trips for each bus line $h \in H$, i.e., $|R^g|$, not all the trips have to be used. Conversely, the model aims at obtaining good headways and offset within the minimum and maximum specified headways' bounds, i.e., Hd_h^{min} and Hd_h^{max}.

The utmost time interval that passengers are willing to wait before boarding line j, subsequent to alighting from line i and traversing to the relevant stop of line j at transfer zone b, is designated as W_b^{ij}. Then, it is considered that two trips, one of line i and the other of line j, are synchronized when the following conditions hold: (i) passengers are able to alight from line i and reach the second bus stop in time to catch the trip of line j; (ii) the waiting time for these passengers at the bus stop awaiting the transfer is less than or equal to W_b^{ij}; and (iii) both of the previous conditions occur within the defined planning period.

With these elements, the MILP model formulation can be presented as follows:

$$\max \quad FO_t = \sum_{b\in B} \sum_{h,g\in H} \sum_{r\in R^h, r>1} \sum_{s\in R^g} \left(z_{rsb}^{hg} \cdot \frac{Dem_b^{hg} \times (x_r^h - x_{r-1}^h)}{T} \right) \tag{1}$$

$$\min \quad FO_c = \sum_{h\in H} Co^h \cdot \left(\sum_{r\in R^h} q_r^i \right) \tag{2}$$

$$\text{s.t.} \quad z_{rsb}^{hg} \leq 1 + \frac{(a_{rb}^h + Wd_b^{hg} + Tol_b^{hg}) - a_{sb}^g}{BigM}, \quad \begin{array}{l}\forall\, h,g \in H, r \in R^h, \\ s \in R^g, b \in B\end{array} \tag{3}$$

$$z_{rsb}^{hg} \leq 1 + \frac{a_{sb}^g - (a_{rb}^h + Wd_b^{hg})}{BigM}, \quad \begin{array}{l}\forall\, h,g \in H, r \in R^h, \\ s \in R^g, b \in B\end{array} \tag{4}$$

$$a_{rb}^h = x_r^h + TT_b^h, \quad \begin{array}{l}\forall\, h \in H, r \in R^h \\ b \in B,\end{array} \tag{5}$$

$$\sum_{s\in R^g} z_{rsb}^{hg} \leq 1, \quad \begin{array}{l}\forall\, h,g \in H, r \in R^h, \\ b \in B\end{array} \tag{6}$$

$$\frac{T+1-x_r^h}{T+1} \leq q_r^h, \quad \forall\, h \in H, r \in R^h \tag{7}$$

$$q_r^h \leq 1 + \frac{T - x_r^h}{N}, \quad \forall\, h \in H, r \in R^h \tag{8}$$

$$z_{rsb}^{hg} \leq q_s^g, \quad \begin{array}{l}\forall h,g \in H, r \in R^h, \\ s \in R^g, b \in B\end{array} \tag{9}$$

$$\sum_{r\in R^h} q_r^h \geq N_h, \quad \forall\, h \in H \tag{10}$$

$$Hd_h^{min} \leq x_r^h - x_{r-1}^h, \quad \begin{array}{l}\forall\, h \in H, \\ r \in R^h, r > 1\end{array} \tag{11}$$

$$x_r^h - x_{r-1}^h \leq Hd_h^{max}, \quad \begin{array}{l}\forall\, h \in H, \\ r \in R^h, r > 1\end{array} \tag{12}$$

$$0 \leq x_0^h \leq Hd_h^{max}, \quad \forall\, h \in H \tag{13}$$

$$z, q \in \{0,1\},\ x, a \geq 0 \tag{14}$$

The objective function outlined in Equation (1) aims at maximizing the demand fulfilled by the successful transfers throughout the planning period by considering the transfer between all the trips of any pair of bus lines in all the transfer zones. The demand is calculated under the assumption of uniform distribution in the planning horizon and thus is directly proportional to the interval of time between two consecutive trips ($x_r^h - x_{r-1}^h$) as long as a successful transfer was achieved ($z_{rsb}^{hg} = 1$). The objective function (2) aims at minimizing the cost of the system in which each bus line is multiplied by a cost parameter Co^h estimated with the cost model described in Section 2.3. Clearly, both objective functions represent conflicting goals. In the pursuit of increasing the number of possible transfers, it becomes necessary to schedule a greater number of trips of the bus lines, thereby escalating the overall system cost. Conversely, opting for a more reduced cost of the system by scheduling only a limited number of trips may lead to challenges in effectively synchronizing successful transfers. Regarding Constraints, Constraint (3) enforces z_{rsb}^{hg} to take value 0 whenever passengers should wait longer than Tol_b^{hg} at transfer zone $b \in B$ before the next trip of bus line $g \in H$ arrives (i.e., when a successful transfer is not achieved). $BigM$ is a sufficiently large value to prevent the right-hand side from becoming negative. Constraint (4) forces z_{rsb}^{hg} to be 0 if passengers

from trip $r \in R^h$ of line $h \in H$ do not have enough time to walk to the subsequent bus stop at zone $b \in B$ to board the $s \in R^g$ of line $g \in H$. Constraint (5) calculates the auxiliary variable a^h_{rb}, which indicates the arrival time of trip $r \in R^h$ of bus line $h \in H$ to transfer zone $b \in B$, adding the travel time to the zone to the departure time.

The characterization of synchronization events with z^{hg}_{rsb} variables deserves further elaboration. Figure 2 shows a hypothetical synchronization attempt, where a passenger on the r-th bus on line h alights at some stop with the intention of boarding the next bus on line g. Let us assume that the picture spans the entire transfer zone b, that is, there are only two stops involved. The time at which this passenger arrives at the first stop is $a^h_{rb} = x^h_r + TT^h_b$: the result of adding the departure time of the bus r (x^h_r) with the travel time TT^h_b is necessary for that bus to move from the departure station until transshipment zone b.

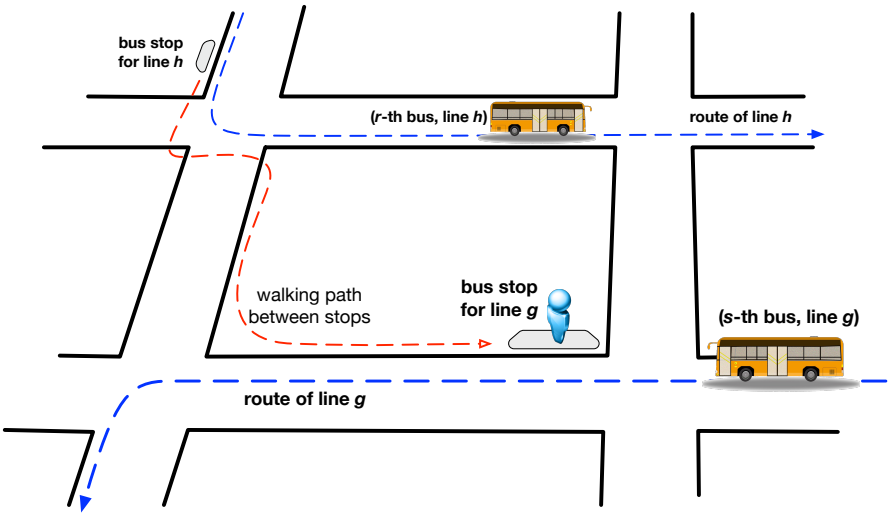

Figure 2. Actors and entities of a synchronization event with the path of vehicles and users indicated in dashed blue and red lines, respectively.

In the example above, the boarding stop is different from the first, so the passenger has to walk to the other stop to catch the next bus, which requires a walking time Wd^{hg}_b. Those situations where both stops are one (i.e., there is no need to walk) can be modeled by setting $Wd^{hg}_b = 0$. Once the passenger arrives at the bus stop for line g, they take the following bus, namely the s-th bus of that line, which arrives at time $a^g_{sb} = x^g_s + TT^g_b$. Both arrival times are computed by means of constraint (5).

Observe that in Equation (1), since variables z^{hg}_{rsb} are factors multiplying positive values ($0 < Hd^{min}_h \leq x^h_r - x^h_{r-1}$ because of Equation (11)), the optimization itself is going to push z^{hg}_{rsb} values upwards, so z^{hg}_{rsb} are to be 1 whenever they allowed for it. When the arrival time a^g_{sb} of bus s surpasses the time at which the passenger reaches the second stop ($a^h_{rb} + Wd^{hg}_b$), plus the waiting tolerance (Tol^{hg}_b), Equation (3) prohibits z^{hg}_{rsb} from having a value of 1. In addition, the bus s cannot be taken by the passenger when the bus arrives at the stop (a^g_{sb}) earlier than the passenger itself ($a^h_{rb} + Wd^{hg}_b$), a case that is covered by Equation (4). It is possible yet that more than one bus (s_1, s_2, etc.) could satisfy Equations (3) and (4). Since the passenger is only to take one bus, constraint (6) sets that the number of transfers between two trips of two bus lines in the same transfer zone cannot be counted more than once.

Constraint (7) forces q^h_r to be 1 when the trip $r \in R^h$ of bus line $h \in H$ is to be scheduled (within the planning horizon). Only the trips that are scheduled with a departing time within the planning horizon (i.e., less than or equal to T) are considered valid trips and are counted in the solution. Complementary, Constraint (8) forces q^h_r to be 0 when a trip is scheduled with a departing time beyond the planning horizon, i.e., $h^h_r > T$; thus, it is not

part of the solution. To summarize, only those trips scheduled with a departing time within the planning horizon are considered valid. The trips scheduled beyond this time are unused trips for that bus line. Whenever the s-th trip of $g \in H$ (i.e., $s \in R^g$) is not to be scheduled, passengers from any other trip $r \in R^h$ at any zone $b \in B$ cannot transfer to it. The last fact is captured by Constraint (9). The values for N_h with $h \in H$ are the result of the QoS model in Section 2.2. For every line h in the system, Constraint (10) schedules—at least—the minimum number of trips required to statistically prevent congestion. Constraints (11) and (12) impose the time interval between two consecutive trips of the same bus line (i.e., the headway) to fall within the predefined boundaries of Hd_h^{min} and Hd_h^{max}, respectively. Similarly, Constraint (13) enforces that the first trip of each bus line $h \in H$ in the planning horizon, i.e., x_1^h, departs in the interval $[0, Hd_h^{max}]$. Finally, Constraints (14) succinctly assert the nature of the variables.

The presence of products $z_{rsb}^{hg}(x_r^h - x_{r-1}^h)$ in the objective function renders the formulation akin to a Mixed-Integer Quadratic Programming (MIQP) problem. Addressing non-linear programming presents a distinct challenge compared to linear problems, usually requiring a larger amount of computational resources [38,39]. To tackle this issue, the variable transformation proposed by [40] is used. Let us define y_{rsb}^{hg} as $z_{rsb}^{hg}(x_r^h - x_{r-1}^h)$. After the redefinition of variables, the linear objective becomes $\frac{\sum_{b\in B}\sum_{h,g\in H}\sum_{r\in R^h}\sum_{s\in R^g} y_{rsb}^{hg}\cdot Dem_b^{hg}}{T}$. To ensure equivalence between the original objective and the modified version, two equations are added for each y_{rsb}^{hg} variable: (i) $y_{rsb}^{hg} \leq (x_r^h - x_{r-1}^h)$ and (ii) $y_{rsb}^{hg} \leq Hd_h^{max} \cdot z_{rsb}^{hg}$.

It is important to highlight that within a maximization context, variables y_{rsb}^{hg} strive to attain the highest possible value. Thus, the third restriction of method proposed by [40]—to force y_{rsb}^{hg} to adopt value $(x_r^h - x_{r-1}^h)$ when $z_{rsb}^{hg} = 1$—is not necessary. In this manner, the introduced variable transformation renders the problem linear, akin to Mixed Integer Linear Programming (MILP), alleviating the computational complexities associated with quadratic terms.

2.5. Related Work

The topic of bus timetabling has been explored in various studies with different criteria [26]. The most commonly considered optimization objectives include minimizing user waiting time as well as the required number of buses for providing the service or the total travel time of buses, and maximizing the occupation of buses. Only a few works have addressed the optimization of bus frequencies to enhance synchronization between buses or with other modes of transportation [26]. Improving synchronization involves designing trip schedules that ensure buses arrive at transfer zones at convenient times that facilitate users to take other buses in the zone. A convenient transfer should achieve a balance by ensuring that waiting times are brief to enhance passenger Quality of Service (QoS), while also being sufficiently long to enable passengers to transfer smoothly from one line to another [25]. Consequently, the Synchronization Bus Problem aims to determine the departing time for each trip of each bus line in a network in order to maximize the number of successful transfers in synchronization nodes. Additionally, due to its computational complexity, there is a scarcity of research that employs exact methods to solve the Bus Synchronization Problem (BSP). The computational complexity was proved for both single-objective [26] and multi-objective versions of the problem [41].

As far as we are concerned, there is no work that addresses the multi-objective bus synchronization problem with a multi-objective exact resolution algorithm. However, there are a few works that solved, with exact methods, a single-objective version of the problem. In their work, Ibarra and Rios [42] introduced an exact mathematical formulation of the problem to address small instances. However, due to the computational complexity of the problem, this exact formulation becomes intractable for large instances. Another group of authors that used mathematical formulations for this problem were Fouilhoux et al. [25]. In their formulation, the number of trips per bus line was considered fixed. To strengthen the formulation, they proposed some valid inequalities to strengthen the formulation. They

demonstrated that these valid inequalities offer a stronger formulation of the problem, enabling the solution of instances of practical size that would otherwise be unsolvable with the plain mathematical formulation. In a more comprehensive model, Chu et al. [43] focused on reducing passenger travel time from the start of their journey to their destination as the primary objective, with the synchronization of buses being a subordinate result of this objective. The authors presented two different mathematical formulations: a plain formulation similar to other related works, and a formulation based on set-partitioning. The formulation based on set-partitioning proved to be more competitive to solve larger instances in smaller computing times than the plain formulation. Cortés et al. [44] presented a bus synchronization planning problem that, as a novel feature, considers dwelling times. In operating models, the dwelling time refers to the duration that a bus remains stopped at a bus stop. Despite being an important factor to consider for day-to-day operations management, when it comes to models used in the tactical planning stage of the system, the dwelling time is often not taken into account. The authors proposed a MILP model to obtain the specific timetables and the duration of the dwelling periods of the buses that maximize the number of successful transfers. The model is enhanced via the introduction of some valid inequalities. The computational experimentation is performed in real instances of the transport system of Santiago de Chile, showing that solutions obtained with the model have around 70% more transfers than the current base-case operation. In our previous article [18], we focused on addressing two distinct variants of the Bus Synchronization Problem (BSP) specifically during peak hours. The first variant considered buses of the same line departing at regular intervals, requiring determination of only the offset, i.e., the departure time of the first bus. The second variant allowed for variable headways between consecutive bus departures of the same bus line within given predefined limits. To tackle both variants, we developed an exact MILP formulation. We applied this formulation to real instances retrieved from the bus network of the city of Montevideo. The results significantly outperformed the current schedules used in the city in terms of the number of successful transfers achieved and average waiting times for users. Our proposed schedules demonstrated clear improvements over the existing schedules, highlighting the efficacy of our approach.

Among the authors that addressed this problem with heuristic methods is the work of Wu et al. [41], who proposed a multi-objective optimization model for the bus synchronization problem to obtain solutions which simultaneously balance the objectives of maximizing the number of successful transfers and minimize the deviation from the departure times of the previous timetable. This is performed in order to acknowledge the impact that the redesign of the timetable of the existing schedule can have on the usual trip plans of passengers. They addressed the problem using a non-dominated sorting genetic algorithm (NSGA-II) as a solution approach and performed a computational experimentation in instances based on the city of Shenyang, China. Elbaz et al. [45] addressed a synchronization problem to maximize the number of synchronized buses and minimize the total waiting time of users. As a resolution strategy, they combined an evolutionary algorithm and a multi-agent system to alternate between the intensification and diversification phases of the metaheuristic. No computational experimentation is performed.

Another relevant aspect discussed in the related literature is the behavior of different stakeholders when bus transport parameters are varied, primarily focusing on which parameters can affect the demand of users for the service [46]. For instance, Ali et al. [47] proposed a unified model as a bi-level optimization problem. In the upper level, the fare of the bus operator is optimized, constrained with bus frequency. In the lower level, the travel costs of commuters are minimized as a sub-assignment traffic model. Simulations are conducted for studying how demand varies according to different bus ticket fares to determine tradeoffs that attain benefits for both users and the public transport company. Similar to the model proposed in this work, Canca et al. [48] studied the captured demand depending on the frequency of the transport unit (in this case, the train transport network). Additionally, they studied the behavior of demand given different levels of government

subsidies to the ticket fare. The more frequent the transport units depart, the more demand is captured, but the larger the cost of the system. Additionally, Wirasinghe [49] studied a bus network feeding an urban train line, analyzing how demand varies depending on the distance of users to the bus stop, which serves as a proxy for the accessibility of the system. Dou and Meng [50] presented a similar work in which not only the departure times of buses are optimized but also the bus capacity in terms of the number of users to be transported.

This article makes a valuable contribution by presenting a formulation based on mathematical programming for the timetable synchronization problem that, unlike previous approaches, considers a multi-objective perspective that aims to maximize the number of successful transfers for passengers undertaking multi-leg trips, while simultaneously minimizing the cost of the system based on a specific cost model. This objective, incorporating a cost model, has not been explored in previous multi-objective versions of the problem. Furthermore, the proposed model takes into account specific constraints related to the Quality of Service (QoS), which are essential for ensuring a satisfactory level of service for passengers. Additionally, different from the usual practice in the related literature, the article employs an exact resolution algorithm to address this bi-objective problem. This algorithm allows for the solution of realistic instances of the problem.

Overall, this article offers a comprehensive and innovative approach to the timetable synchronization problem, introducing a multi-objective perspective considering the cost of the system, taking into account specific QoS constraints, and employing an exact resolution algorithm for realistic instances.

3. Resolution Methodology

In multi-objective optimization, it is not possible to find a unique optimal solution that simultaneously optimizes all the objective functions [51]. Thus, the goal is to identify a set of efficient solutions that cannot be compared mathematically and demonstrate the tradeoff between two objectives. Specifically, in bi-objective minimization problems, a solution vector s^* within the feasible space S is considered a non-dominated or efficient solution if there is no other solution $s \in S$ that is strictly better, i.e., simultaneously holds $f_1(s) \leq f_1(s^*), f_2(s) \leq f_2(s^*)$ and $f_i(s) < f_i(s^*)$ for some objective i (where $f_i(s)$ is the objective function of objective i evaluated on solution s). For example, Figure 3 illustrates a bi-objective minimization problem. In this depiction, solution c is evidently dominated by solutions a, b, and d, as these three solutions exhibit superior values in both objectives. Subsequently, solution d is dominated by solution a since, despite having the same value for f_2, solution a excels in terms of objective f_1. Finally, solutions a and b emerge as non-dominated solutions, with neither being preferable over the other based on the provided information. The set of non-dominated or efficient solutions is the Pareto frontier.

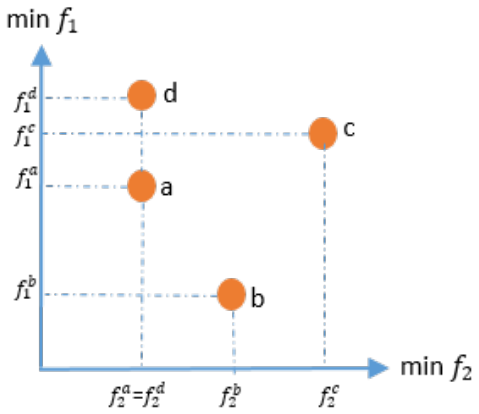

Figure 3. Example of non-dominated solutions in a bi-objective minimization problem.

The most commonly used methods for handling multi-objective problems are the weighting or weighted-sum method and the ε-constraint method. These methods need to be executed multiple times to find in each run a non-dominated solution and iteratively construct the Pareto front. However, the weighting method usually requires a larger number of runs as many of them can result in repeated solutions. Additionally, this method cannot reach solutions located in non-convex regions of the Pareto front [51,52]. In this work, the ε-constraint method [53] is chosen to address the target problem. This selection is based on the evidence in the related literature that has been successfully applied in other similar bi-objective problems related to transport planning. For example, Cervantes et al. [54] solved a bi-objective optimization problem for the transit network design of public transport while minimizing the travel times and the monetary costs of users and while also considering the cost of the system as a constraint. They implemented the ε-constraint method, which was able to obtain approximations of the Pareto front for benchmark instances based on benchmark instances developed by Mandl [55] in reasonable computing times. Moreover, the ε-constraint method allowed them to study the tradeoff among both objectives, leading to relevant information for the decision-making process. Guerriero et al. [56] used the ε-constraint to addressed a Dial-a-Ride public transport problem in which the customer requires a delivery to be made specifying the place of pickup (origin) and delivery (destination), time windows for the pickup and the delivery, and the quantity of a certain product that has to be transported. The model aims at assigning vehicles for the required trips while minimizing the maximum total ride time and the total waiting time for customers. The model is applied over benchmark instances [57]. Finally, in another transport planning problem, Ko and Song [58] applied the ε-constraint method to design the route of a CityTour Bus service, minimizing the total investment cost and CO_2 emissions. Their study, focused on the city of Seoul, effectively explored the tradeoff among objectives, showcasing the versatility and applicability of the ε-constraint method in diverse transport planning scenarios.

In bi-objective optimization, the ε-constraint method consists of solving a single-objective optimization problem considering only one objective function, while the other objective is limited in an additional constraint. In a minimization (maximization) problem, in this additional constraint, the objective function is forced to be smaller than (greater than) the certain parameter ε. Then, the method obtains different non-dominated solutions to approximate the Pareto front by performing several runs with different values of ε, which successively modifies the feasible region of the problem. The modification of the feasible region is illustrated in Figure 4, representing an optimization problem with the objective to minimize f_1 and maximize f_2. From left to right, the process begins by obtaining the solution with the maximum value of f_2 (f_2^{Max}), representing an extreme point on the Pareto front. Subsequently, two intermediate non-dominated solutions are obtained using parameters ε and ε′ to restrict the objective f_2 and thereby modify the feasible region. Finally, in the last step, f_2 is restricted to its minimal value f_2^{Min}, further restricting the feasible region. In this last step, the solution with the minimal value f_2 is obtained, representing another extreme point on the Pareto front.

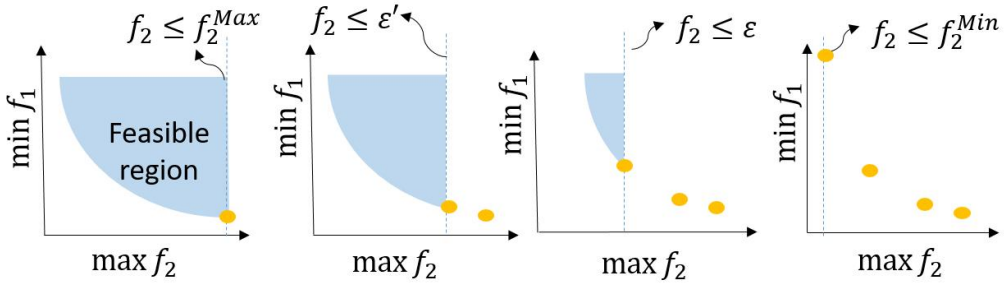

Figure 4. Example of the modification of the feasible region of the problem in successive runs of the ε-constraint method in a bi-objective problem.

The application of the ε-constraint method is performed as is described in Algorithm 2. First, it starts by calculating the extreme solutions. To calculate the extreme solution with the maximum number of transfers, a single-objective model is solved considering only the objective of the number of transfers FO_t (as in Equation (1)) (line 1 of Algorithm 2). The obtained solution is added as the first solution of the Pareto front (line 2) and the maximum value of the cost of the system within the Pareto front $maxC$ is retrieved from this solution (line 3). Similarly, to obtain the extreme solution with minimal cost, a single-objective model is solved considering only the objective of the cost of the system FO_c as in Equation (2) (line 4 in Algorithm 2). The obtained solution is added as the first solution of the Pareto front (line 5) and the minimum value of the cost of the system within the Pareto front $minC$ is retrieved from this solution (line 6). Then, the $step$ for the variation in ε is calculated by considering the two extreme values of the cost and the number of efficient solutions which are aimed to obtain n (line 7). For launching the iterative process to obtain the rest of the solutions of the Pareto front, the ε is initially set to the minimum cost value (line 8). Afterwards, the iterative process for constructing the Pareto front is performed (lines 9–12). In each iteration of this process, a single-objective problem is solved which aims at maximizing the number of transfers FO_t subjected to both the constraints of the problem (Equations (3)–(13)) and an additional constraint, which forces the cost to be smaller or equal to ε ($F_c \leq \varepsilon$) (line 10) in order to obtain an efficient solution. The obtained solution is added to the Pareto front (line 11) and the ε is incremented with the $step$ (line 12) for the next iteration. Notably, the use of the minimum cost to initialize ε (line 8) is different from which is usually performed when applying the ε-constraint method. Usually the ε is initialized with the worst value of the restricted objective [59], in the case of this problem, the maximum cost. Initializing the ε with the worst value of the restricted objective allows for the iterative process to start with a problem which is relatively easy to solve and, by moving the ε towards the best value of the restricted objective, progressively incriminates the complexity of the successive problems in each iteration (with the restricted objective forced to reach values nearer to the best attainable value). However, in this case, using the minimum cost as the initial value of the ε allows the solution of the problem of the previous iteration to be a feasible solution of the problem of the next iteration and, thus, can be used as a *warm start* via the solver for the new problem. The warm start can be advantageous as it assists CPLEX in narrowing down the search space and allows it to use heuristics, which require a feasible solution right from the beginning of the search [60]. In preliminary experiments, it was found that the *warm start* significantly improved the performance of the solver for the problem addressed in this paper.

Algorithm 2 ε-constraint method for bus synchronization problem

Input: Instance, n

1: $(FO_c^*, FO_t^*) \leftarrow$ Solve $\max\{FO_t | Equations\ (3)–(13)\}$
2: $ParetoFront \leftarrow (FO_c^*, FO_t^*)$
3: $maxC \leftarrow FO_c^*$
4: $(FO_c^*, FO_t^*) \leftarrow$ Solve $\min\{FO_c | Equations\ (3)–(13)\}$
5: $ParetoFront \leftarrow ParetoFront \cup (FO_c^*, FO_t^*)$
6: $minC \leftarrow FO_c^*$
7: $step \leftarrow \frac{maxC - minC}{n-1}$
8: $\varepsilon \leftarrow minC$
9: **for** $\{i \leftarrow 0; i \leq n; i++\}$ **do**
10: $\quad (FO_c^*, FO_t^*) \leftarrow$ Solve $\max\{FO_t | Equations\ (3)–(13) \cup F_c \leq \varepsilon\}$
11: $\quad ParetoFront \leftarrow ParetoFront \cup (FO_c^*, FO_t^*)$
12: $\quad \varepsilon \leftarrow \varepsilon + step$

Output: $ParetoFront$

4. Results

This section provides an overview of the application of the proposed model on real-world instances of the city of Montevideo. It includes the implementation details, a description of the instance set used, as well as the report and analysis of the obtained numerical results.

4.1. Implementation Details and Execution Platform

The MILP formulation for the bus synchronization problem was coded and solved with IBM ILOG CPLEX Interactive Optimizer 12.6.3.0. To facilitate the process, a program in C was used to translate the instances from the .csv format to the LP-format that CPLEX uses. The pre-processing and post-processing of the obtained solutions was performed in Matlab (version R2015a-8.5.0). Additionally, Matlab was also used to develop the discrete event simulation model for estimating bus occupation as described in Section 2.2.

The experiments were conducted on an HP ProLiant DL380 G9 high-end server equipped with two Intel Xeon Gold 6138 processors, each having 20 cores and a RAM memory of 128 GB. The computing resources were provided via the high-performance computing infrastructure of the National Supercomputing Center, Uruguay (Cluster-UY [61]).

4.2. Description of Instances

For the computational experimentation, 25 instances were created using real data from Montevideo. Various sources of information were utilized to build these instances. Details about the route of bus lines, the schedules, and the location of bus stops were obtained from the National Open Catalog of Uruguay. The information about transfers was provided by the City Hall of Montevideo and was processed using the urban data analysis methodology proposed in [21]. The planning horizon was set to the rush hour at midday in Montevideo, which is from 12:00 to 14:00 [3].

To construct the instances, the demand function was derived from the information of the smart cards ticket sales' database. The transfer zones were selected based on demand, i.e., pairs of bus stops with the highest number of registered transfers during the specified period. Then, the considered bus lines are those that pass through these synchronization points. Each instance included information from 30, 70, and 100 transfer zones, chosen randomly from the 170 most demanded transfer zones in the city. The time traveling function, denoted as TT, for each bus line was empirically computed using GPS data. The walking time between bus stops was estimated by considering a walking speed of 6 km/h and the distance between bus stops within each transfer zone, which was obtained using geospatial information about the stops.

For each instance, different levels of Quality of Service (QoS) provided to the citizens were used. The different levels of QoS were modeled with different values of the parameter Tol_b^{hg}, which represents the maximum threshold time that users are willing to wait for a transfer from bus line $h \in H$ to bus line $g \in H$. This parameter was set as λHd_g^{max}, where λ took values from the range [0.5, 0.7, 0.9, 1] and Hd_h^{max} is the maximum bound for the headway of the bus line $g \in H$. This allowed for the consideration of different thresholds of user tolerance regarding the time they are willing to wait. The problem instances were named in the format NL.λ.id, where NL represented the number of bus lines, λ was the percentage coefficient applied to the waiting time of the line (representing different thresholds of tolerance), and id is an identifier for differentiating instances with the same NL and λ.

4.3. Numerical Results

In this section, we present the main results of the application of the MILP model to the set of instances.

4.3.1. Distance of the Best Trade-Off Solution to the Ideal Vector

In Table 2, the distance between the ideal vector, representing an unattainable solution characterized by the best objective values across all executions, and the best trade-off or compromising solution is presented for each instance. The best trade-off solution is the efficient solution that has the smallest (Euclidean) normalized distance to the ideal vector within the space of the objectives [62], as depicted in Figure 5. To find the best trade-off solution, distances to the ideal vector are computed using the expression of the overall deviation provided in Equation (15).

$$\Delta = \sqrt{\sum_{o \in O} \left(\frac{value_o - ideal_o}{ideal_o} \right)^2} \tag{15}$$

Since Pareto fronts usually consist of multiple solutions, summary metrics are necessary. In this context, it is common to analyze the best trade-off solution as one of the suitable candidate solutions for implementation in the real problem, since it is the solution that better balances the fulfillment of all the objectives [63]. The expression computes the overall normalized Euclidean distance of a solution to the ideal vector. To obtain this value, each objective is normalized with the ideal value. Thus, the solution with the minimal deviation Δ is chosen as the best trade-off solution.

Moving from left to right, Table 2 reports the percentage difference from the ideal vector for the number of transfers (δ_t), the percentage difference from the ideal vector for the cost of the system (δ_c), and lastly, the comprehensive overall deviation Δ.

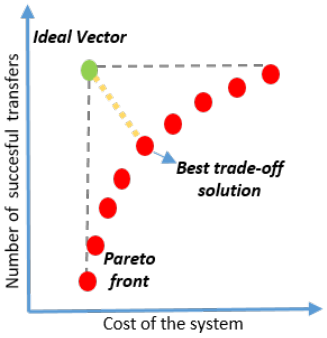

Figure 5. Ideal vector and best trade-off solution.

Table 2. Distances of the best trade-off solution to the ideal vector.

Instance	Successful Transfers			Cost			Δ
	Ideal	Trade-Off	δ_T	Ideal	Trade-Off	δ_T	
37.100.1	312.77	308.30	1.43%	6346.24	6346.24	0.00%	1.43%
37.30.1	309.44	301.37	2.61%	6348.56	6470.94	1.93%	3.24%
37.50.1	311.76	303.17	2.76%	6346.57	6453.30	1.68%	3.23%
37.70.1	310.81	305.60	1.68%	6344.95	6344.95	0.00%	1.68%
37.90.1	312.60	308.21	1.40%	6339.61	6339.61	0.00%	1.40%
40.100.0	246.14	245.01	0.46%	6188.41	6312.70	2.01%	2.06%
40.100.4	273.10	268.17	1.81%	6106.75	6159.77	0.87%	2.00%
40.30.0	242.72	236.93	2.39%	6193.28	6293.08	1.61%	2.88%
40.30.4	264.70	255.06	3.64%	6103.68	6281.73	2.92%	4.67%
40.50.0	247.69	240.08	3.07%	6193.28	6280.23	1.40%	3.38%
40.50.4	272.71	266.12	2.42%	6106.75	6272.04	2.71%	3.63%
40.70.0	247.62	243.23	1.77%	6188.41	6320.16	2.13%	2.77%
40.70.4	274.18	266.86	2.67%	6103.68	6269.77	2.72%	3.81%
40.90.0	249.03	244.10	1.98%	6191.48	6297.10	1.71%	2.61%

Table 2. *Cont.*

Instance	Successful Transfers			Cost			Δ
	Ideal	Trade-Off	δ_T	Ideal	Trade-Off	δ_T	
40.90.4	273.52	268.57	1.81%	6103.68	6177.02	1.20%	2.17%
41.100.2	289.12	287.72	0.48%	7052.32	7199.76	2.09%	2.15%
41.30.2	284.95	273.22	4.12%	7052.32	7212.24	2.27%	4.70%
41.50.2	286.95	277.29	3.37%	7052.32	7170.65	1.68%	3.76%
41.70.2	290.47	285.84	1.59%	7052.32	7219.65	2.37%	2.86%
41.90.2	290.82	285.14	1.95%	7052.32	7137.91	1.21%	2.30%
42.100.3	277.42	272.06	1.93%	7642.51	7642.51	0.00%	1.93%
42.30.3	270.57	264.93	2.08%	7644.06	7773.12	1.69%	2.68%
42.50.3	275.31	268.87	2.34%	7643.71	7788.25	1.89%	3.01%
42.70.3	276.38	273.92	0.89%	7643.40	7794.86	1.98%	2.17%
42.90.3	277.76	271.58	2.22%	7633.18	7633.18	0.00%	2.22%
Average			2.11%			1.52%	2.75%

Analyzing the results of the distance between the ideal solution and the solution with the best tradeoff is shown in Table 2, where it can be concluded that the MILP model is able to obtain, in general, accurate solutions for most of the instances. The average overall deviation is just 2.75%. Moreover, the average of the percentage difference for each particular objective is also low (i.e., 2.11% and 1.52% for the number of transfers and the cost of the system, respectively). When the instances are grouped according to an increasing λ, it can be depicted that in general, δ_T, δ_C and Δ tend to be reduced. The exception is δ_C when λ goes from 90 to 100. This information can be visually depicted in Figure 6.

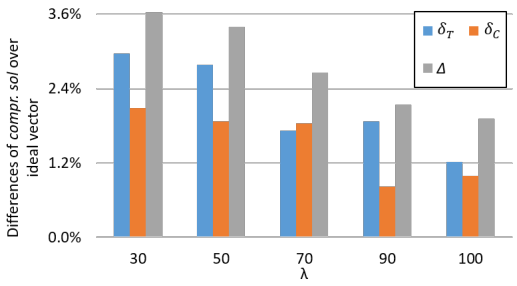

Figure 6. Distance of the best trade-off solution and the ideal vector per λ.

4.3.2. Comparison with the Current Timetables

To establish a meaningful baseline for comparison, the timetables that are currently used in Montevideo, hereafter current timetables (CT), are used. The enhancement of the best trade-off MILP solutions in comparison to the CT is analyzed via metrics: (i) the count of transfers, as stipulated in objective function (1); (ii) the cost of the bus schedule, calculated as per the objective function (2); and (iii) the number of buses used in the solution (Q_r^i). Despite not being an optimization criteria of the MILP model, the number of buses was reported because it is a relevant result for the operational management of the system. The results stemming from the MILP model and the comparison with the Montevideo CT are presented in Table 3. The table reports the values of the CT and the percentage of improvement achieved via both the compromising solution and the extreme solution of the MILP approach for each objective. Notably, the extreme solution that is compared is different when evaluating each objective. The extreme solution is the solution with the largest number of transfers when assessing the number of transfers, whereas it is the solution with the lowest cost when evaluating the cost of the system. Regarding the number of buses, the CT is compared with the compromising solution of the MILP model.

Table 3. Comparison between MILP solutions vs. current timetable (CT).

Instance	Succesful Transfers			Cost			Number of Buses	
	CT	%impr. Comp. sol.	%impr. Extreme sol.	CT	%impr. Comp. sol.	%impr. Extreme sol.	CT	%impr. Comp. sol.
37.100.1	263.41	17.04%	18.74%	8721.80	27.24%	27.24%	439	13.21%
37.30.1	110.4	172.98%	180.29%	8721.80	25.81%	27.21%	439	3.87%
37.50.1	175.67	72.58%	77.47%	8721.80	26.01%	27.23%	439	5.24%
37.70.1	236.18	29.39%	31.60%	8721.80	27.25%	27.25%	439	−1.82%
37.90.1	263.41	17.01%	18.67%	8721.80	27.31%	27.31%	439	11.16%
40.100.0	209.02	17.22%	17.76%	8592.64	26.53%	27.98%	419	1.91%
40.100.4	226.72	18.28%	20.46%	8717.53	29.34%	29.95%	428	17.29%
40.30.0	92.19	157.00%	163.28%	8592.64	26.76%	27.92%	419	6.68%
40.30.4	106.48	139.54%	148.59%	8717.53	27.94%	29.98%	428	9.81%
40.50.0	136.12	76.37%	81.96%	8592.64	26.91%	27.92%	419	5.25%
40.50.4	134.54	97.80%	102.70%	8717.53	28.05%	29.95%	428	12.15%
40.70.0	184.56	31.79%	34.17%	8592.64	26.45%	27.98%	419	14.80%
40.70.4	198.87	34.19%	37.87%	8717.53	28.08%	29.98%	428	17.76%
40.90.0	209.02	16.78%	19.14%	8592.64	26.72%	27.94%	419	15.27%
40.90.4	224.82	19.46%	21.66%	8717.53	29.14%	29.98%	428	17.76%
41.100.2	244.42	17.72%	18.29%	10,056.59	28.41%	29.87%	471	14.01%
41.30.2	102.65	166.17%	177.59%	10,056.59	28.28%	29.87%	471	18.26%
41.50.2	158.69	74.74%	80.82%	10,056.59	28.70%	29.87%	471	20.38%
41.70.2	213.11	34.13%	36.30%	10,056.59	28.21%	29.87%	471	8.92%
41.90.2	243.96	16.88%	19.21%	10,056.59	29.02%	29.87%	471	19.53%
42.100.3	228.3	19.17%	21.52%	10,410.35	26.59%	26.59%	485	13.20%
42.30.3	98.26	169.62%	175.36%	10,410.35	25.33%	26.57%	485	7.63%
42.50.3	150.73	78.38%	82.65%	10,410.35	25.19%	26.58%	485	18.56%
42.70.3	203.04	34.91%	36.12%	10,410.35	25.12%	26.58%	485	13.40%
42.90.3	227.72	19.26%	21.97%	10,410.35	26.68%	26.68%	485	8.45%
Average		61.94%	65.77%		27.24%	28.33%		11.71%

Overall, the solutions obtained via the MILP approach are significantly superior than the CT, particularly in terms of successful transfers. The average improvement of the compromising solution over the CT in terms of successful transfers is 61.94% for all the instances, achieving the greatest improvement in instance 37.30.1 (172%). Similarly, the extreme solution excels the CT in terms of successful transfers of 65.77% on average, obtaining the best improvement also in instance 37.30.1 (180.29%). Regarding the costs of the system, the improvements of the best trade-off solution over the CT are on average 27.24%, with the greatest improvement on instance 40.100.4 (29.34%). The extreme solution excels the CT on average by 28.33% in terms of costs of the system, obtaining the best improvement simultaneously in three instances with forty bus lines, i.e., instances 40.30.4, 40.70.4, and 40.90.4 (29.98%). In the case of the number of buses, the compromising solutions use on average 11.71% less buses than the CT, achieving the maximum reduction in instance 41.50.2 (20.38%). Only in instance 37.70.1 does the compromising solution of the MILP model use a slightly larger number of buses (1.82% larger). From these results, when compared to CT, it can be observed that the MILP approach is particularly efficient in generating schedules that excel in terms of the number of successful transfers. However, the MILP approach is also able to improve the cost of the system as well. This dual benefit underscores the versatility and effectiveness of MILP in optimizing public transportation schedules, striking a favorable balance between passenger convenience and cost effectiveness.

When the instances are grouped per λ, it can be depicted that the higher λ is, the smaller the improvement of the compromising and extreme solutions in terms of successful transfer

(Figure 7a). This pattern can be associated such that, when the tolerable waiting time of users is smaller, the model has a smaller gap for synchronizing buses schedules to achieve successful transfers. Regarding the number of successful transfers, the average percentage improvement via the MILP model goes from 161.06% when $\lambda = 30$ to 17.89% when $\lambda = 100$ regarding the compromising solution. Similarly, the average percentage improvement of the extreme solution goes from 169.00% when $\lambda = 30$ to 19.40% when $\lambda = 100$ regarding the compromising solution. On the other hand, the increment of λ affects less the capacity of the MILP model to obtain solutions with better costs, as is depicted in Figure 7b. The average percentage improvement of the cost of the system via the MILP model goes from 26.83% when $\lambda = 30$ to 27.64% when $\lambda = 100$ regarding the compromising solution. Moreover, the average percentage improvement of the extreme solution remains almost fixed around 28.33% for any value of λ.

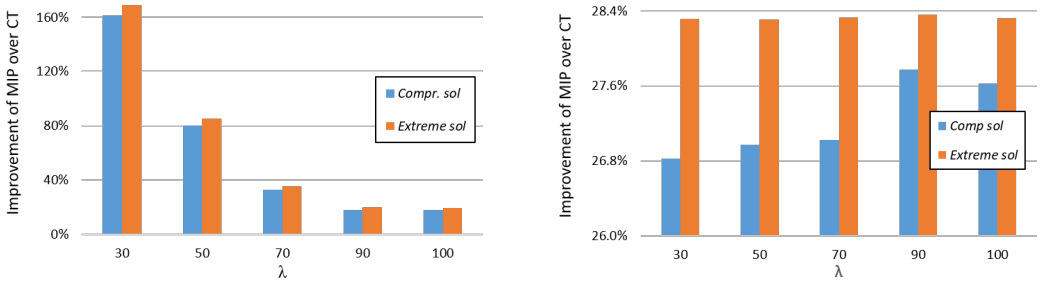

(**a**) (**b**)

Figure 7. Average percentage improvement of the MILP model over CT for each value of λ. (**a**) Number of successful transfers. (**b**) Cost of the system.

4.3.3. Representative Pareto Fronts

As a graphic presentation of the general results, Figure 8 is introduced. In this figure, the consolidated Pareto fronts are presented for four representative instances. From these figures, it can be observed that the MILP model is able to compute a set of solutions that efficiently explore the tradeoff among objectives. The model is also able to compute solutions in non-convex regions of the Pareto front that, as aforementioned, is an advantage of the selected resolution approach (ε-constraint method) over other traditional approaches, such as the weighted sum.

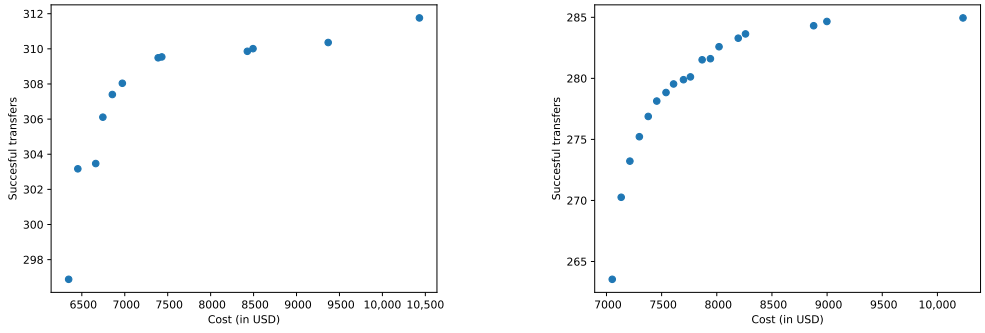

(**a**) (**b**)

Figure 8. *Cont.*

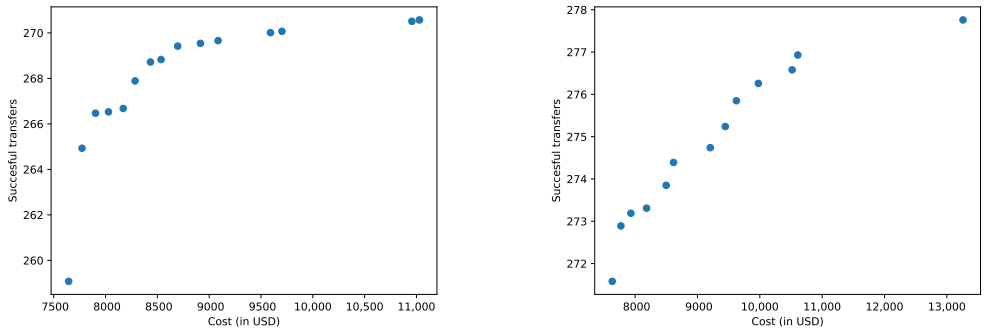

(**c**) (**d**)

Figure 8. Pareto fronts of representative instances. (**a**) Pareto front of instance 40.30.4, (**b**) Pareto front of instance 41.30.2, (**c**) Pareto front of instance 42.30.3, and (**d**) Pareto front of instance 42.90.3.

5. Conclusions

The smart cities paradigm involves the aim of developing more interconnected and sustainable urban environments. Within this aim, the enhancement of public transport systems is crucial for facilitating citizens to commute without using private cars. Since it is impossible to provide users with direct connections to every location of the city, an aspect that should be carefully planned when operating the public transport system is the synchronizations among different bus lines. In this line, this article introduced a novel Mixed-Integer Linear Programming (MILP) model for bus timetabling with a focus on enhancing the multi-leg trip while ensuring a minimum level of quality of service for passengers. As a second objective, the MILP model also aims at minimizing the cost of the system.

The performance of the MILP model was assessed using a set of real-world instances from the public bus system of Montevideo, Uruguay. The set of instances included instances with different numbers of bus lines and different required levels of quality of service represented by the maximum tolerable waiting time for transferring passengers. The results showcased the competitiveness of the MILP model to provide a range of Pareto efficient solutions that explore the tradeoff between the number of successful transfers of passengers and system costs. Moreover, the results demonstrated the superiority of the MILP solutions over the existing timetables used in Montevideo, specially in terms of the number of successful transfers, but also in terms of the costs of the system. Particularly, the model excelled in terms of successful transfers, with an average percentage improvement of 65.77% for the best trade-off solution. It also demonstrated cost efficiency, with an average improvement of 27.24% for the best trade-off solution over the current timetable. Additionally, the results revealed that the capacity of the MILP model to synchronize bus schedules is amplified when passengers are willing to wait longer, leading to significant gains in the number of successful transfers obtained in solutions when the maximum tolerable waiting time is increased.

Currently, our proposed approach has certain limitations that could be enhanced in various aspects to model a broader range of realistic public transport systems. This includes incorporating hybrid and electric buses and adopting a more advanced bus occupation model. Therefore, regarding future work, there are several promising directions related to addressing these limitations. One is the incorporation of electric or hybrid buses into the model to include more sustainable practices that are being implemented worldwide. This would involve introducing new control variables to assess the feasibility and benefits of using these types of buses on specific lines as well as developing new cost models for these types of buses. This would involve introducing new control variables (to evaluate the feasibility and benefits of using this type of bus on specific lines) and developing new cost models for this type of bus. Another line of research is improving the Quality of Service (QoS) model in relation to the occupancy of buses during direct trips. The approach

followed in this article combines random boarding with deterministic passengers alighting. The first hypothesis is a standard assumption for arrival processes, but a stochastic alighting process is a more realistic approximation. The bus occupancy simulator can be extended to incorporate additional information, such as intelligent methods for inferring where passengers alight the bus [21]. Another relevant line for future work is evaluating the proposed algorithmic approach in a real setting, applying a microscopic traffic simulator and using real traffic information for public and private transportation. Finally, another research line is to use different integer solvers to address the problem in order to compare CPLEX performance.

Finally, while our paper proposed an efficient methodology for optimizing bus timetabling in public transportation systems, a more in-depth discussion on the practical implications of our proposed solutions and their real-world implementation is also a relevant future research line. To bridge the gap between theory and practical application, it is important to analyze the potential challenges and limitations that may arise during this transition. For instance, the accuracy of travel time estimations, the reliability of bus occupation models, and the appropriateness of cost considerations in real-world scenarios need careful scrutiny. By addressing these practical aspects, our proposed solutions can be better tailored to meet the dynamic demands and constraints of real-world public transportation systems, ensuring their feasibility and effectiveness in implementation.

Author Contributions: Conceptualization, C.R., S.N. and D.R.; methodology, C.R., S.N. and D.R.; data curation, S.N.; validation, C.R.; formal analysis, C.R. and D.R.; investigation, C.R., S.N. and D.R.; resources, C.R. and S.N.; software, C.R.; supervision, C.R., S.N. and D.R.; writing—original draft, D.R.; writing—review and editing, C.R., S.N. and D.R.; visualization, D.R. All authors have read and agreed to the published version of the manuscript.

Funding: This work was partially supported by PEDECIBA (Programa de Desarrollo de las Ciencias Básicas), Uruguay.

Institutional Review Board Statement: Not applicable.

Informed Consent Statement: Not applicable.

Data Availability Statement: The data presented in this study are available on request from the corresponding author. The data are not publicly available due to privacy concerns.

Conflicts of Interest: The authors declare no conflict of interest.

References

1. Grava, S. *Urban Transportation Systems: Choices for Communities*; McGraw-Hill: New York, NY, USA, 2002.
2. Deakin, M.; Al Waer, H. From intelligent to smart cities. *Intell. Build. Int.* **2011**, *3*, 140–152. [CrossRef]
3. Nesmachnow, S.; Hipogrosso, S. Transit oriented development analysis of Parque Rodó neighborhood, Montevideo, Uruguay. *World Dev. Sustain.* **2022**, *1*, 100017. [CrossRef]
4. Tolley, R. (Ed.) *Sustainable Transport*; Woodhead Publishing: Sawston, UK, 2003.
5. Hipogrosso, S.; Nesmachnow, S. Analysis of sustainable public transportation and mobility recommendations for Montevideo and Parque Rodó neighborhood. *Smart Cities* **2020**, *3*, 479–510. [CrossRef]
6. Poudenx, P. The effect of transportation policies on energy consumption and greenhouse gas emission from urban passenger transportation. *Transp. Res. Part A Policy Pract.* **2008**, *42*, 901–909. [CrossRef]
7. Bıyık, C.; Abareshi, A.; Paz, A.; Ruiz, R.A.; Battarra, R.; Rogers, C.D.; Lizarraga, C. Smart Mobility Adoption: A Review of the Literature. *J. Open Innov. Technol. Mark. Complex.* **2021**, *7*, 146. [CrossRef]
8. Beirão, G.; Cabral, J. Understanding attitudes towards public transport and private car: A qualitative study. *Transp. Policy* **2007**, *14*, 478–489. [CrossRef]
9. Takamatsu, M.; Taguchi, A. Bus timetable design to ensure smooth transfers in areas with low-frequency public transportation services. *Transp. Sci.* **2020**, *54*, 1238–1250. [CrossRef]
10. Ceder, A.; Wilson, N. Bus network design. *Transp. Res. Part B Methodol.* **1986**, *20*, 331–344. [CrossRef]
11. Ceder, A. Methods for creating bus timetables. *Transp. Res. Part A Gen.* **1987**, *21*, 59–83. [CrossRef]
12. Chowdhury, S.; Giacaman, N. En-Route Planning of Multi-Destination Public-Transport Trips Using Smartphones. *J. Public Transp.* **2015**, *18*, 31–45. [CrossRef]
13. Ceder, A.; Tal, O. Timetable Synchronization for Buses. In *Lecture Notes in Economics and Mathematical Systems*; Springer: Berlin/Heidelberg, Germany, 1999; pp. 245–258.

14. Ma, H.; Li, X.; Yu, H. Single bus line timetable optimization with big data: A case study in Beijing. *Inf. Sci.* **2020**, *536*, 53–66. [CrossRef]
15. Xu, X.; Yu, Y.; Long, J. Integrated electric bus timetabling and scheduling problem. *Transp. Res. Part C Emerg. Technol.* **2023**, *149*, 104057. [CrossRef]
16. Massobrio, R.; Nesmachnow, S.; Muraña, J.; Dorronsoro, B. Learning to optimize timetables for efficient transfers in public transportation systems. *Appl. Soft Comput.* **2022**, *119*, 108616. [CrossRef]
17. Nesmachnow, S.; Muraña, J.; Goñi, G.; Massobrio, R.; Tchernykh, A. Evolutionary Approach for Bus Synchronization. In *Communications in Computer and Information Science*; Springer International Publishing: Berlin/Heidelberg, Germany, 2020; pp. 320–336.
18. Nesmachnow, S.; Risso, C. Exact and Evolutionary Algorithms for Synchronization of Public Transportation Timetables Considering Extended Transfer Zones. *Appl. Sci.* **2021**, *11*, 7138. [CrossRef]
19. Intendencia de Montevideo. Sistema de Transporte Metropolitano. Available online: https://montevideo.gub.uy/areas-tematicas/sistema-de-transporte-metropolitano (accessed on 3 August 2023).
20. Intendencia de Montevideo. Sistema de Información Geográfica. Available online: https://sig.montevideo.gub.uy/ (accessed on 3 August 2023).
21. Massobrio, R.; Nesmachnow, S. Urban mobility data analysis for public transportation systems: A case study in Montevideo, Uruguay. *Appl. Sci.* **2020**, *10*, 5400. [CrossRef]
22. Intendencia de Montevideo. Observatorio de Movilidad, Transporte Público. Available online: http://montevideo.gub.uy/observatorio-de-movilidad/transporte-publico[05/2023] (accessed on 3 August 2023).
23. Brands, T.; de Romph, E.; Veitch, T.; Cook, J. Modelling Public Transport Route Choice, with Multiple Access and Egress Modes. *Transp. Res. Procedia* **2014**, *1*, 12–23. [CrossRef]
24. Risso, C.; Nesmachnow, S. Optimized design of a backbone network for public transportation in Montevideo, Uruguay. *Sustainability* **2023**, *15*, 16402. [CrossRef]
25. Fouilhoux, P.; Ibarra, O.; Kedad, S.; Rios, Y. Valid inequalities for the synchronization bus timetabling problem. *Eur. J. Oper. Res.* **2016**, *251*, 442–450. [CrossRef]
26. Ibarra, O.; Delgado, F.; Giesen, R.; Muñoz, J. Planning, operation, and control of bus transport systems: A literature review. *Transp. Res. Part B Methodol.* **2015**, *77*, 38–75. [CrossRef]
27. Kim, S.H.; Whitt, W. Choosing arrival process models for service systems: Tests of a nonhomogeneous Poisson process. *Nav. Res. Logist. (NRL)* **2014**, *61*, 66–90. [CrossRef]
28. Lancia, C.; Lulli, G. Predictive modeling of inbound demand at major European airports with Poisson and Pre-Scheduled Random Arrivals. *Eur. J. Oper. Res.* **2020**, *280*, 179–190. [CrossRef]
29. Intendencia de Montevideo. Sistema de Transporte Metropolitano, Tarifas. Available online: https://montevideo.gub.uy/areas-tematicas/sistema-de-transporte-metropolitano/tarifas-del-transporte-colectivo-urbano (accessed on 3 August 2023).
30. Marquez, G. Informe Sobre Tarifas y Subsidios a Usuarios del Sistema de Transporte Público de Pasajeros de Montevideo. 2019. Available online: https://montevideo.gub.uy/sites/default/files/biblioteca/imsubsidiosaltransportedigital.pdf (accessed on 8 August 2023).
31. Avenali, A.; Boitani, A.; Catalano, G.; D'Alfonso, T.; Matteucci, G. Assessing standard costs in local public bus transport: A hybrid cost model. *Transp. Policy* **2018**, *62*, 48–57. [CrossRef]
32. Mehran, B.; Yang, Y.; Mishra, S. Analytical models for comparing operational costs of regular bus and semi-flexible transit services. *Public Transp.* **2020**, *12*, 147–169. [CrossRef]
33. Mishra, S.; Mehran, B.; Sahu, P. Assessment of delivery models for semi-flexible transit operation in low-demand conditions. *Transp. Policy* **2020**, *99*, 275–287. [CrossRef]
34. Taylor, B.; Garrett, M.; Iseki, H. Measuring cost variability in provision of transit service. *Transp. Res. Rec.* **2000**, *1735*, 101–112. [CrossRef]
35. Sinner, M.; Weidmann, U.; Nash, A. Application of a cost-allocation model to Swiss bus and train lines. *Transp. Res. Rec.* **2018**, *2672*, 431–442. [CrossRef]
36. Cherwony, W.; Mundle, S. Peak-base cost allocation models. *Transp. Res. Rec.* **1978**, *663*, 52–56.
37. Cherwony, W.; Gleichman, G.; Porter, B.; Hamilton, B. *Bus Route Costing Procedures: A Review*; Urban Mass Transportation Administration: Washington, DC, USA, 1981.
38. Glover, F.; Woolsey, E. Converting the 0-1 polynomial programming problem to a 0-1 linear program. *Oper. Res.* **1974**, *22*, 180–182. [CrossRef]
39. Miettinen, K. *Nonlinear Multiobjective Optimization*; Springer Science & Business Media: New York, NY, USA, 1999; Volume 12.
40. Glover, F. An improved MIP formulation for products of discrete and continuous variables. *J. Inf. Optim. Sci.* **1984**, *5*, 69–71. [CrossRef]
41. Wu, Y.; Yang, H.; Tang, J.; Yu, Y. Multi-objective re-synchronizing of bus timetable: Model, complexity and solution. *Transp. Res. Part C Emerg. Technol.* **2016**, *67*, 149–168. [CrossRef]
42. Ibarra, O.; Rios, Y. Synchronization of bus timetabling. *Transp. Res. Part B Methodol.* **2012**, *46*, 599–614. [CrossRef]
43. Chu, J.; Korsesthakarn, K.; Hsu, Y.; Wu, H. Models and a solution algorithm for planning transfer synchronization of bus timetables. *Transp. Res. Part E Logist. Transp. Rev.* **2019**, *131*, 247–266. [CrossRef]

44. Cortés, C.; Gil, C.; Gschwender, A.; Rey, P. The bus synchronization timetabling problem with dwelling times. *Transp. Res. Part B Methodol.* **2023**, *174*, 102773. [CrossRef]
45. Elbaz, H.; Alaoui, A.; Bencheikh, G. The synchronization bus timetabling problem, modeling and resolution by the multi-agent approach. In Proceedings of the 2018 4th International Conference on Logistics Operations Management (GOL), Le Havre, France, 10–12 April 2018; pp. 1–6.
46. Parbo, J.; Nielsen, O.A.; Prato, C.G. User perspectives in public transport timetable optimisation. *Transp. Res. Part C Emerg. Technol.* **2014**, *48*, 269–284. [CrossRef]
47. Ali, N.; Nakayama, S.; Yamaguchi, H. Analysis of Bus Fare Structure to Observe Modal Shift, Operator Profit, and Land-Use Choices through Combined Unified Transport Model. *Sustainability* **2021**, *14*, 139. [CrossRef]
48. Canca, D.; De-Los-Santos, A.; Laporte, G.; Mesa, J. Integrated railway rapid transit network design and line planning problem with maximum profit. *Transp. Res. Part E Logist. Transp. Rev.* **2019**, *127*, 1–30. [CrossRef]
49. Wirasinghe, S. Nearly optimal parameters for a rail/feeder-bus system on a rectangular grid. *Transp. Res. Part A Gen.* **1980**, *14*, 33–40. [CrossRef]
50. Dou, X.; Meng, Q. Feeder bus timetable design and vehicle size setting in peak hour demand conditions. *Transp. Res. Rec.* **2019**, *2673*, 321–332. [CrossRef]
51. Deb, K.; Sindhya, K.; Hakanen, J. Multi-objective optimization. In *Decision Sciences*; CRC Press: Boca Raton, FL, USA, 2016; pp. 146–179.
52. Emmerich, M.T.; Deutz, A.H. A tutorial on multiobjective optimization: Fundamentals and evolutionary methods. *Nat. Comput.* **2018**, *17*, 585–609. [CrossRef]
53. Haimes, Y. On a bicriterion formulation of the problems of integrated system identification and system optimization. *IEEE Trans. Syst. Man Cybern.* **1971**, *3*, 296–297.
54. Cervantes, K.; Chavez, M.; Ibarra, O. Analyzing the trade-off between minimizing travel times and reducing monetary costs for users in the transit network design. *Transp. Res. Part B Methodol.* **2023**, *173*, 142–161. [CrossRef]
55. Mandl, C.E. Evaluation and optimization of urban public transportation networks. *Eur. J. Oper. Res.* **1980**, *5*, 396–404. [CrossRef]
56. Guerriero, F.; Pezzella, F.; Pisacane, O.; Trollini, L. Multi-objective optimization in dial-a-ride public transportation. *Transp. Res. Procedia* **2014**, *3*, 299–308. [CrossRef]
57. Li, H.; Lim, A. A metaheuristic for the pickup and delivery problem with time windows. In Proceedings of the Proceedings 13th IEEE International Conference on Tools with Artificial Intelligence, ICTAI 2001, Dallas, TX, USA, 7–9 November 2001; pp. 160–167.
58. Ko, Y.; Song, B. Sustainable service design and revenue management for electric tour bus systems: Seoul city tour bus service and the eco-mileage program. *J. Sustain. Tour.* **2019**, *27*, 308–326. [CrossRef]
59. Rossit, D.; Toutouh, J.; Nesmachnow, S. Exact and heuristic approaches for multi-objective garbage accumulation points location in real scenarios. *Waste Manag.* **2020**, *105*, 467–481. [CrossRef]
60. IBM. ILOG CPLEX Optimization Studio User Manual. Available online: https://www.ibm.com/docs/en/icos/20.1.0?topic=cplex-users-manual (accessed on 3 August 2023).
61. Nesmachnow, S.; Iturriaga, S. Cluster-UY: Collaborative scientific high performance computing in Uruguay. In *Communications in Computer and Information Science, Proceedings of the International Conference on Supercomputing in Mexico, Monterrey, Mexico, 25–29 March 2019*; Springer: Cham, Switzerland, 2019; pp. 188–202.
62. Marler, R.T.; Arora, J.S. Survey of multi-objective optimization methods for engineering. *Struct. Multidiscip. Optim.* **2004**, *26*, 369–395. [CrossRef]
63. Coello, C.; Van Veldhuizen, D.; Lamont, G. *Evolutionary Algorithms for Solving Multi-Objective Problems*; Kluwer Academic: New York, NY, USA, 2002.